Nineteenth Indian Expedition to Antarctica, Scientific Report, 2004
Department of Ocean Development, Technical Publication No. 17, pp 1-19

Geology and Geochemistry of Nunataks Southeast of Schumacher Oasis, cDML, East Antarctica

A.V. Keshava Prasad, M.J. Beg and Arun Chaturvedi

Geological Survey of India, Antarctica Division, Faridabad

Abstract

A dominantly gneissic terrain with enclaves of charnockite and granulite and thin lamprophyre dykes form the lithology of the four nunataks lying southeast of Schirmacher Oasis. While an alternating sequence of orthogneiss (biotite gneiss, biotite-hornblende gneiss) and para-gneiss (garnet- and garnet-biotite-sillimanite gneiss) is exposed in Baalsrudfjellet and Starheimtind nunataks. Para-gneisses are conspicuosly absent in the Sonstebynuten and Pevikhornet nunataks.

Analytical data and various chemical plots thereof, of the orthogneiss and charnockites show that they are igneous in nature while the garnet sillimanite gneisses have sedimentary parentage. The chamockites have low to moderate REE contents while the gneisses have comparatively higher REE contents. The variation diagrams of these rocks show clear trend of the progressive evolution of parent magma from charnockite to gneiss. This is corroborated by the R1-R2 plot of Batchelor-Bowden (1985) wherein the charnockite which occur as enclaves within the ortho-gneiss cluster in the pre-plate collision setting while the host gneisses plot in the syn-collisional field. Considering the similarity of lithological set up and proximity to Schirmacher Oasis, the four nunataks are presumed to be just extensions of the Schirmacher itself.

Introduction

The Antarctic Continent is broadly divided in to West Antarctica and East Antarctica based on their distinct geological set up. The geology of the E. Antarctic craton is dominated by the Archaean-Proterozoic component (Tingey, 1991). The central Dronning Maud Land (cDML) occupies the central space in this E. Antarctic craton with Rayner complex and Enderby land to the east, and western Dronning Maud Land (wDML) to the west. While high-grade metamorphic Archaean component dominates the Rayner complex, the granulite grade metamorphites with abundant of metasediments characterize the wDML set up. The cDML thus holds the key to unravel the evolution of the E. Antarctic craton.

The cDML is predominantly Grenvillian gneissic terrain (with abundant charnockitic and granulitic enclaves) which has been intruded extensively by the Pan-African magmatic activity whose composition ranged from anorthosites to granites with lots of minor gabbroic, lamprophyric and pegmatitic dykes completing the set up(D'Souza *et al.,1996).The* exposure of these rock suites are seen in the Schirmacher Oasis off Princess Astrid coast,farther south in theWohlthat-Humboldt-Orvin Muhlig Hofmann Mountain ranges and the numerous nunataks lying in between.

Geology

A group of four nunataks Baalsrudfjellet,Starheimtind,Sonstebynuten and Pevikhornet, occur 30 km to southeast of Schirmacher Oasis (Fig.1). The board lithology of these nunataks was first document by Mukerji

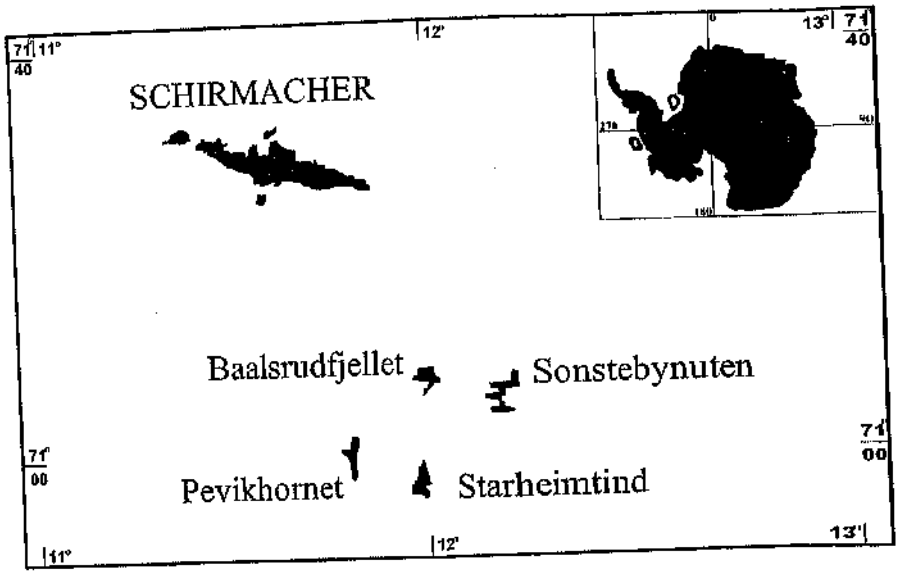

Fig. 1: Location map of the four nunataks geologically mapped during the 19^{1h} Indian Antarctic Expedition

et al (1988). Of these, Baalsrudfjellet and Starheimtind are similar in their lithological set up-Ortho-gneiss and garnet-sillimanite-gneiss are present, while in the Sonstebynuten (Fig. 2) and Pevikhornet nunataks, garnet-sillimanite-gneiss is conspicuous by its absence.

Fig. 2: Panoramic view of Sonstebynuten, one of the four nunataks, south-east of Schirmacher Oasis.

Baalsrudfjellet and Starheimtind: An alternating sequence of Ortho-gneiss (biotite gneiss, gamet-bioite gneiss, biotite-hornblende gneiss) and para-gneiss (biotite-sillimanite gneiss) is exposed in this nunatak (Fig. 3). The general trend is ENE-WSW with steep southerly to sub-vertical dips.

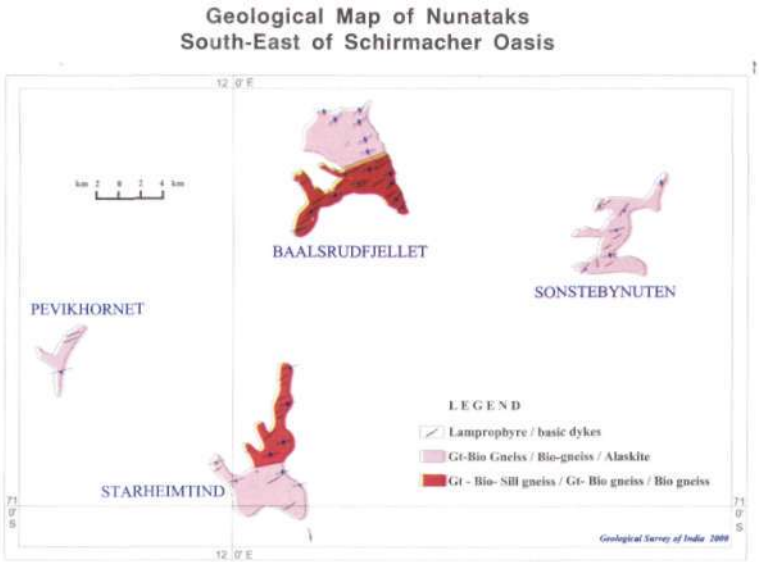

Fig. 3: Geological map of the four nunataks, south-east of Schirmacher Oasis.

Fig. 4: Enclave of charnockite in the host orthogneiss in the nunatak Baalsrudfjellet.

Numerous enclaves of charnockites (Fig. 4) and granulites are present. At many places, these enclaves have a very coarse to medium grained garnet-rich rim. Lamprophyres, pegmatites and gabbroic dykes intrude the country rock. The lamprophyres in particular occur as dyke swarms, trending NE-SW with steep southerly to sub-vertical dips and 20-60 cm wide and are traceable usually up to 50-60 m length. They have sharp contacts with the host rocks.

Sonstebynuten and Pevikhornet: Ortho-gneiss with charnockitic and granulitic enclaves and thin lamprophyre dykes form the lithology of Sonstebynuten and Pevikhornet nunataks (Fig. 3). The general trend is ENE-WSW with steep southerly to subvertical dips.

Rock types and Petrography

Ortho-gneiss: Different variation of ortho-gneiss—biotite-gneiss and biotite-hornblende gneiss are exposed in Baalsrudfjellet Starheimtind and Sonstebynuten. They are medium to coarse grained, show perfect compositional banding and occasionally augen structure. In thin sections, biotite is usually phlogopite, yellowish brown to brownish red. Hornblende shows yellowish to greenish pleochroic colours. Biotite and hornblende usually define foliation (Fig. 5). Secondary biotite forming at the expense of primary hornblende grains with concomitant release of opaques, mostly

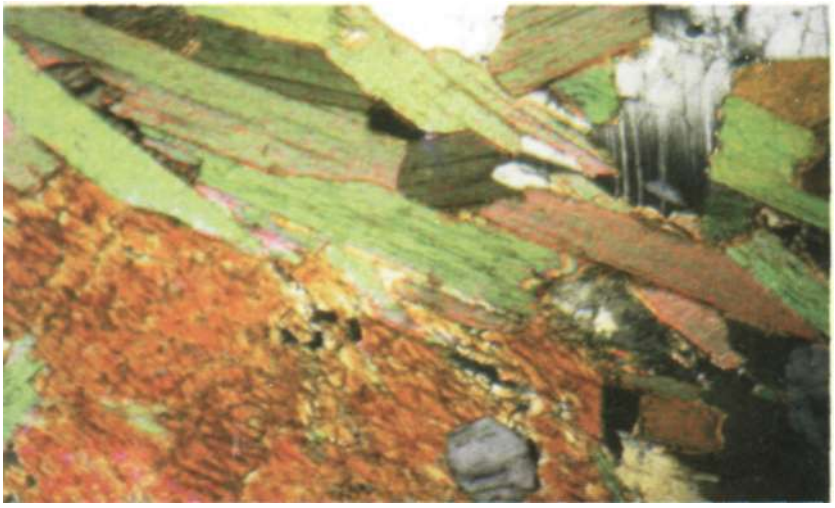

Fig. 5: Biotite and hornblende grains defining foliation in the hbl-bio-bearing orthogneiss from the nunatak Sonstebynuten (crossed nicols; 10x).

magnetite is quite common (Fig. 6). Plagioclase is sodic in nature and orthoclase and microcline form the K-feldspar component. In the augen geniss, well-developed augens of K-feldspars with foliation wrapped around is seen. Zircon and apatite form the accessory mineral assemblage.

Fig. 6: Secondary biotite forming at the expense of hornblende with concomitant exsolution of opaques in the hbl-bio-bearing orthogneiss from Baalsrudfjellet (plane polarized light; 10x).

Garnet-Sillimanite-Gneiss: As stated earlier, the sillimanite bearing gneiss occurs in Baalsrudfjellet and Starheimtind only, while garnet-biotite gneiss and garnet-gneiss (Alaskite)—are exposed in Baalsrudfjellet, Starheimtind and Sonstebynuten. In Pevikhornet, the garnet bearing gneiss is conspicuously absent. The garnet-sillimanite-gneiss shows well developed compositional banding and foliation. The mineral assemblage is garnet-biotite-sillimanite-feldspars-quartz. Garnet is reddish/pinkish brown, euhedral to subrounded and rarely contains inclusion of other minerals. Quite often, garnet grains are surrounded by biotite-chlorite rich rim (Fig. 7). Sillimanite occurs as fine needles and as thick blades measuring up to 2 cm by 4 cm. On the foliation plane, both biotite and sillimanite are randomly oriented. In thin section, sillimanite occurs as needles and prisms, colourless and show medium to high interference colours.

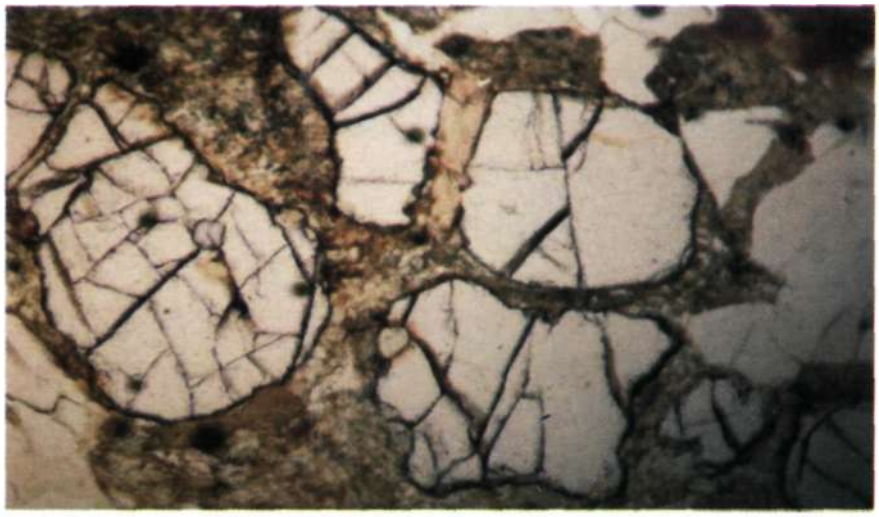

Fig. 7: Garnet grains surrounded by secondary chlorite and biotite rim in gar-bio-bearing orthogneiss from Starheimtind (plane polarized light; 10x).

Charnockite: Occurs as dark greenish grey and greasy, medium to fine grained, weakly foliated and occasionally showing gneissic banding. It occurs as enclaves, sometimes with a garnet-rich mafic rim around it, with-in the host gneiss. Under microscope, these usually show typical granuloblasts texture with grains having triple-point contacts. Biotite and hypersthene form the mafic assemblage. Plagioclase dominates the feldspathic component, thus making the charnockite enderbitic in composition.

Lamprophyre dykes: Lamprophyres are the most common intrusives in the area. All the lamprophyres are mesocratic to melanocratic, compact,

fine grained and show porphyritic texture (Keshava Prasad *et al,* 2001). Phenocrysts are uniformly distributed and no zonation is observed. The dominant phenocryst biotite is set in greenish grey to dark grey matrix. Ocellar structures of 1-3 mm across are observed in the lamprophyres of Baalsrudfjellet. The lamprophyres from Baalsrudfjellet show two distinct phenocryst assemblages—biotite-clinopyroxene and biotite-clinopyroxene-olivine, while in lamprophyres from Sonstebynuten nunatak, biotite-clinopyroxene and biotite-clinopyroxene-hornblende assemblages are observed. The lamprophyres from Starheimtind nunatak have only biotite-clinopyroxene assemblage and the nunatak Pevikhornet has lamprophyres with biotite-hornblende-clinopyroxene assemblage.

In general, in the lamprophyres of the nunataks mapped, it is observed that biotite is of phlogopite variety and amphibole, wherever present is common hornblende. It is yellowish green to pale green. Diopside and augite make up the clinopyroxene population; ocelli are mainly feldspathic and epidotisation is less. Most of the ocelli are elongated and all of them have delimiting biotites. Biotite, clinopyroxene feldspars and minor amounts of free quartz constitute the matrix assemblage. Compositionally these lamprophyres are calc-alkaline in nature. Detailed chemistry and petrogenesis of these lamprophyres is being published separately.

Geochemistry

Whole rock analysis of all the samples was carried out at PPOD Laboratory of AMSE-GSI, Bangalore, using Phillips XRF instrument. The Trace Element analysis was done using ICP-AES at Chemical Laboratory, GSI, Faridabad and Rare Earth Elements were analyzed using Instrumental Nuetron Activation Analysis Technique at NAA Laboratory at GSI, Pune. The representative analyses along with CIPW norm of charnockite and ortho-gneiss are given in Tables 1 and 2, respectively.

The $Si0_2$ content of the orthogneiss ranges from 62.71 to 71.05 wt% while $A1_20_3$ ranges from 12.95 to 14.99. The FeO (total) content is between 2.51 and 8.02 wt% while total Alkali content is between 5.71 and 8.04 wt%. In contrast, $Si0_2$ in charnockite ranges from 48.91 to 55.87 wt% and $A1_20_3$ from 11.95 to 15.61 wt%. The Fe-Mg values are quite high, which range from 13.99 to 23.89 wt% while alkali content is low—between 2.85 to 4.14 wt%—as compared to the orthogneiss. In the varia-

tion diagram of various oxides, a clear pattern is seen. The charnockite and the orthogneiss define a trend line (Fig. 8). In the TAS plot both the rock types plot in the subalkaline field (Fig. 9) and in the AFM diagram, the

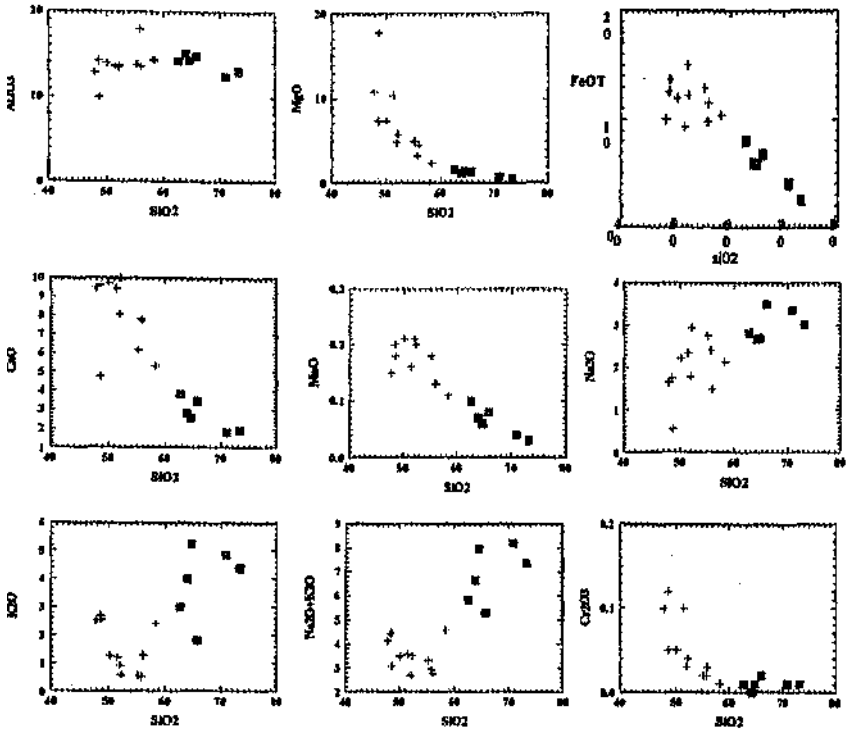

Fig, 8: Harker diagrams for the host ortho gneiss and charnockite enclaves from the nunataks (Symbols: ■ - Orthogneiss; + - Charnockite).

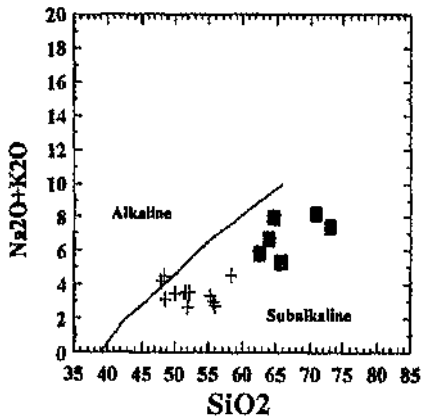

Fig. 9: Variation diagram for the orthogneiss and charnockite showing their sub-alkaline nature.

gneisses have dominantly calc-alkaline trend while charnockites have distinctive tholeiitic trend (Fig. 10). The charnockite samples plot in the igneous field. In the QAP plot of the gneiss and charnockite (Fig. 11), the gneisses

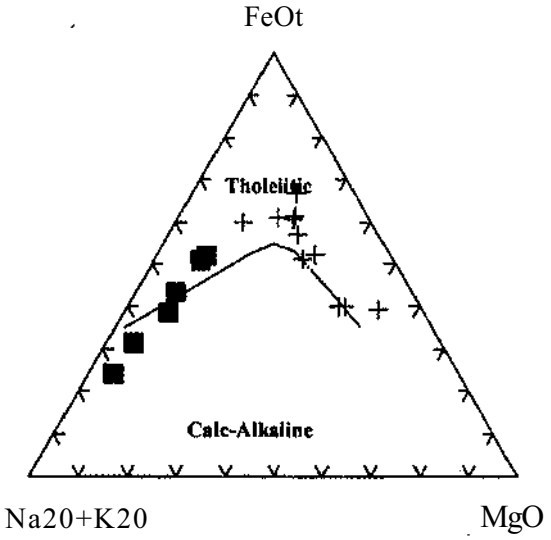

Fig. 10: AFM Diagram for the orthogneiss and the charnockite showing distinct trends.

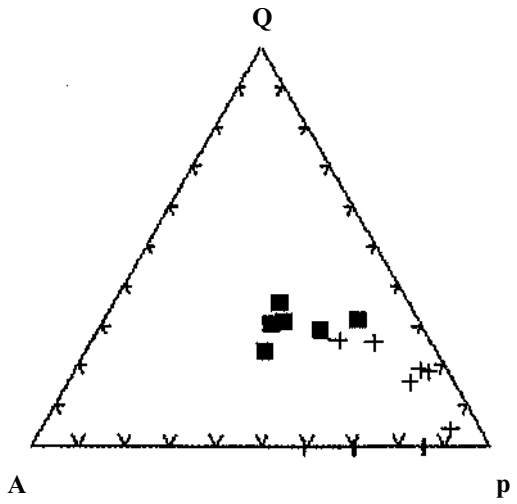

Fig. 11: QAP diagram of normative compositions of the Orthogneiss and Charnockite from the nunataks (Symbols: ■ - Orthogneiss; + - Charnockite).

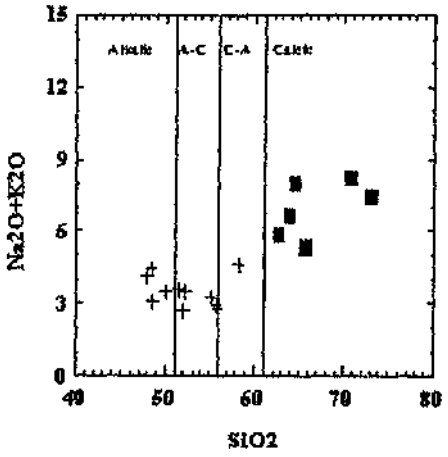

Fig. 12: TAS diagram for the orthogneiss and the charnockite from nunataks.

plot in the monzo-granite to granite fields while the charnockites plot in the granodiorite to monzo-diorite-diorite fields. The total alkali vs. $Si0_2$ plot (Fig. 12) shows that while orthogneiss plot in the calcic field, the charnockite plot in alkaline to calc-alkaline fields.

The charnockites have low to moderate REE contents (S = 17.62-216.69) while the gneisses have comparatively higher REE contents (Σ = 150.11- 475.61). The Chondrite normalized REE plots (Fig. 13) show that both gneiss and charnockite are enriched in LREE as compared to HREE,

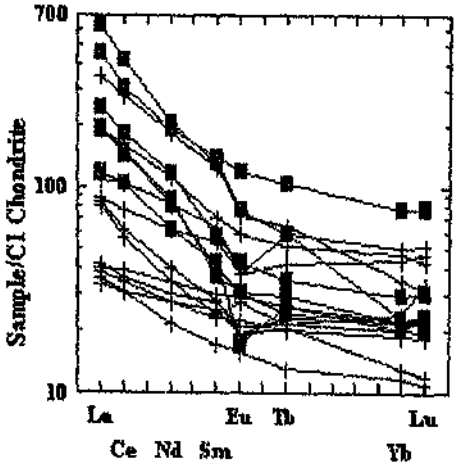

Fig. 13: Chondrite normalized REE pattern for the orthogneiss and charnockite of the nunataks.

Table 1: Composition (Major (Wt%). Trace (ppm) and Rare Earth Elements (ppm)) and of The Selected Charnockite Samples from the Nunataks (Samples from St: Starheimtind; B: Baalsrndfjellet; Sn: Sonstebynuten)

	24/1-ST3	4/2-B2	4/2-B3	5/2-B7	5/2-B7D	6/2-ST55	7/2-B1	7/2-B54	7/2-B9	8/2-SN3	8/2-SN7
SiO_2	52.08	55.69	55.92	50.12	48.54	55.18	51.54	48.66	58.32	52.33	47.93
TiO_2	2.03	1.34	2.38	1.45	1.59	2.35	0.67	0.97	2.64	1.51	1.03
Al_2O_3	13.47	17.94	13.58	13.96	14.26	13.75	13.67	9.95	14.35	13.69	12.93
FeOT	14.99	9.72	11.46	11.91	12.51	12.81	9.29	13.62	10.42	12.21	9.96
MnO	0.21	0.13	0.13	0.21	0.20	0.18	0.16	0.18	0.11	0.20	0.15
MgO	4.81	3.25	4.50	7.37	7.42	5.05	10.36	17.80	2.41	5.73	10.74
CaO	8.09	7.82	7.75	9.73	9.65	6.17	9.44	4.73	5.33	10.00	9.51
Na_20	1.78	2.40	1.48	2.21	1.75	2.74	2.34	0.54	2.14	2.94	1.63
K_2O	0.90	0.52	1.28	1.27	2.68	0.57	1.21	2.54	2.42	0.58	2.51
P_2O_5	0.34	0.17	0.41	0.16	0.20	0.56	0.09	0.16	0.88	0.18	0.54
S	0.04	0.04	0.04	0.04	0.03	0.06	0.04	0.05	0.05	0.05	0.11
Cr_20_3	0.03	0.02	0.03	0.05	0.05	0.02	0.10	0.12	0.01	0.04	0.10
NiO	0.01	0.00	0.00	0.01	0.01	0.00	0.03	0.08	0.00	0.01	0.02
BaO	0.00	0.00	0.00	0.00	0.00	0.00	0.00	0.01	0.02	0.00	0.12
LOI	0.46	0.15	0.39	0.47	0.58	0.00	0.09	0.22	0.11	0.00	1.18
Total	**99.24**	**99.19**	99.35	**98.96**	**99.47**	**99.44**	**99.03**	**99.63**	**99.21**	**99.47**	**98.46**
Li	9.00	14.00	18.00	13.00	22.00	11.00	23.00	9.00	18.00	9.00	31.00
Be	1.00	1.00	1.00	1.00	1.00	1.00	1.00	1.00	1.00	1.00	1.00
B	9.00	9.00	9.00	9.00	9.00	9.00	9.00	9.00	9.00	9.00	9.00
V	329.00	64.00	236.00	265.00	203.00	244.00	124.00	117.00	152.00	256.00	175.00

(Contd)

Table 1: Normative composition of the charnockites from nunataks (Contd..)

	24/1-ST3	4/2-B2	4/2-B3	5/2-B7	5/2-B7D	6/2-ST55	7/2-Bl	7/2-B54	7/2-B9	8/2-SN3	8/2-SN7
Cr	236.00	169.00	258.00	495.00	395.00	221.00	746.00	923.00	104.00	298.00	775.00
Co	38.00	16.00	27.00	42.00	38.00	31.00	34.00	60.00	18.00	31.00	34.00
Ni	100.00	71.00	83.00	88.00	104.00	90.00	224.00	583.00	59.00	66.00	171.00
Cu	25.00	8.00	17.00	33.00	18.00	18.00	5.00	8.00	20.00	18.00	67.00
Zn	154.00	129.00	76.00	121.00	147.00	80.00	86.00	194.00	172.00	114.00	105.00
As	19.00	28.00	19.00	19.00	20.00	19.00	48.00	19.00	19.00	19.00	19.00
Rb	15.00	0.00	30.00	25.00	80.00	9.00	30.00	65.00	25.00	9.00	50.00
Sr	131.00	285.00	111.00	114.00	72.00	292.00	166.00	93.00	496.00	177.00	1043.00
Y	33.00	23.00	58.00	26.00	23.00	71.00	19.00	19.00	54.00	29.00	23.00
Nb	19.00	19.00	26.00	21.00	19.00	36.00	19.00	19.00	49.00	19.00	22.00
Mo	4.00	4.00	4.00	4.00	4.00	4.00	4.00	4.00	4.00	4.00	4.00
Ag	0.90	0.90	0.90	0.90	0.90	0.90	0.90	0.90	0.90	0.90	0.90
Cd	1.00	1.00	1.00	1.00	1.00	1.00	1.00	1.00	1.00	1.00	1.00
Sn	19.00	19.00	19.00	19.00	19.00	19.00	19.00	19.00	19.00	19.00	19.00
Sb	9.00	9.00	9.00	9.00	9.00	9.00	9.00	9.00	9.00	9.00	9.00
Ba	188.00	37.00	9.00	43.00	105.00	103.00	123.00	267.00	1276.00	78.00	1382.00
W	9.00	15.00	14.00	12.00	18.00	13.00	11.00	9.00	17.00	9.00	10.00
Pb	9.00	14.00	9.00	9.00	9.00	9.00	10.00	9.00	11.00	9.00	10.00
Bi	9.00	11.00	9.00	12.00	12.00	9.00	11.00	9.00	9.00	9.00	9.00
Zr	170.00	348.00	288.00	161.00	151.00	226.00	135.00	139.00	556.00	118.00	192.00
Th	0.71	1.90	2.70	1.00	0.50	6.20	1.10	2.20	0.90	0.18	4..30
Sc	**57.00**	**36.00**	**47.00**	**49.00**	40.00	44.00	29.00	30.00	32.00	49.00	31.00

(Contd)

Table 1: Normative composition of the charnockites from nunataks (Contd..)

	24/1-ST3	4/2-B2	4/2-B3	5/2-B7	5/2-B7D	6/2-ST55	7/2-B1	7/2-B54	7/2-B9	8/2-SN3	8/2-SN7
Hf	3.40	6.50	11.00	3.00	2.40	11.00	1.00	3.30	26.00	3.30	3.40
Ta	0.17	0.50	0.75	0.10	0.10	1.10	0.22	0.10	0.65	0.50	0.65
La	9.70	19.00	26.00	8.00	9.00	45.00	8.50	20.00	84.00	10.00	21.00
Ce	24.00	34.00	64.00	19.00	21.00	97.00	19.00	38.00	170.00	22.00	47.00
Nd	16.00	16.00	38.00	13.00	13.00	52.00	10.00	19.00	84.00	14.00	29.00
Sm	4.60	3.70	9.70	3.80	3.50	11.00	2.60	4.30	19.00	4.20	8.20
Eu	1.70	1.60	2.20	1.10	1.30	3.40	0.90	1.10	4.20	1.20	2.20
Tb	1.00	0.80	2.20	0.86	0.75	1.90	0.49	0.77	2.40	0.80	1.60
Yb	3.70	4.10	8.60	3.70	3.20	8.00	2.00	2.20	5.90	3.40	7.60
Lu	0.56	0.85	1.30	0.55	0.47	1.10	0.28	0.30	0.80	0.60	1.20
REETot	61.26	80.05	152.00	50.01	52.22	219.40	43.77	85.67	370.30	56.20	117.80
Q	8.95	13.52	16.60	0.00	0.00	11.94	0.00	0.00	19.34	2.15	0.00
C	0.00	0.00	0.00	0.00	0.00	0.00	0.00	0.00	0.62	0.00	0.00
Or	5.39	3.10	7.65	7.63	16.03	3.39	7.24	15.14	14.44	3.45	15.30
Ab	15.26	20.52	12.66	19.01	14.99	23.33	20.05	4.61	18.29	25.03	14.23
An	26.43	37.00	26.91	24.80	23.40	23.67	23.50	17.36	20.90	22.57	21.19
Ne	0.00	0.00	0.00	0.00	0.00	0.00	0.00	0.00	0.00	0.00	0.00
Lc	0.00	0.00	0.00	0.00	0.00	0.00	0.00	0.00	0.00	0.00	0.00
A	5.39	3.10	7.65	7.63	16.03	3.39	7.24	15.14	14.44	3.45	15.30
P	41.69	57.52	39.57	43.81	38.39	47.00	43.55	21.97	39.19	47.60	35.42
Ac	0.00	0.00	0.00	0.00	0.00	0.00	0.00	0.00	0.00	0.00	0.00
Ns	0.00	0.00	0.00	0.00	0.00	0.00	0.00	0.00	0.00	0.00	0.00

(Contd)

Table 1: Normative composition of the charnockites from mmataks (Contd..)

	24/1-ST3	4/2-B2	4/2-B3	5/2-B7	5/2-B7D	6/2-ST55	7/2-B1	7/2-B54	7/2-B9	8/2-SN3	8/2-SN7
Di	10.05	0.90	7.68	19.03	19.49	2.87	18.83	4.22	0.00	21.68	19.25
DiWo	4.99	0.45	3.86	9.67	9.89	1.44	9.72	2.19	0.00	10.91	9.94
DiEn	1.98	0.18	1.78	5.13	5.18	0.65	6.12	1.44	0.00	5.16	6.27
DiFs	3.08	0.27	2.04	4.24	4.42	0.78	2.99	0.60	0.00	5.60	3.04
Hy	25.86	19.81	20.39	21.04	5.35	26.14	19.15	33.40	16.97	19.06	5.74
HyEn	10.11	7.96	9.50	11.52	2.89	11.95	12.87	23.60	6.04	9.14	3.87
HyFs	15.75	11.85	10.88	9.52	2.47	14.19	6.29	9.79	10.94	9.92	1.87
01	0.00	0.00	0.00	2.58	14.36	0.00	7.57	19.89	0.00	0.00	18.63
OlFo	0.00	0.00	0.00	1.35	7.39	0.00	4.92	13.64	0.00	0.00	12.14
OlFa	0.00	0.00	0.00	1.23	6.97	0.00	2.65	6.25	0.00	0.00	6.49
Mt	3.31	2.14	2.52	2.64	2.76	2.80	2.04	2.98	2.28	2.67	2.23
Hm	0.00	0.00	0.00	0.00	0.00	0.00	0.00	0.00	0.00	0.00	0.00
II	3.91	2.57	4.57	2.80	3.06	4.49	1.29	1.86	5.06	2.89	2.02
Ap	0.75	0.37	0.91	0.36	0.44	1.23	0.20	0.35	1.94	0.40	1.22

Table 2 : Composition (Major (Wt%), Trace (ppm) and Rare Earth Elements (ppm)) of Selected Orthogneiss from the Nunataks

	13/1-P2	25/l-ST8a	4/2-B1	6/2-ST5	7/2-B7	8/2-SN12
$Si0_2$	73.17	62.68	65.83	64.01	64.72	70.87
TiO_2	0.24	1.77	1.13	1.52	1.15	0.48
AL_20_3	13.07	14.22	14.78	15.02	14.31	12.40
FeOT	2.51	8.02	6.85	5.99	5.86	4.06
MnO	0.03	0.10	0.08	0.07	0.06	0.04
MgO	0.53	1.59	1.33	1.16	1.39	0.73
CaO	1.90	3.81	3.45	2.81	2.57	1.81
Na_20	3.01	2.81	3.50	2.67	2.69	3.35
K_20	4.37	3.00	1.80	3.97	5.25	4.84
p_2O_5	0.07	0.73	0.15	0.68	0.44	0.16
S	0.05	0.04	0.04	0.04	0.09	0.02
cr_2O_3	0.01	0.01	0.02	0.00	0.01	0.01
NiO	0.00	0.00	0.01	0.00	0.00	0.00
BaO	0.10	0.00	0.01	0.03	0.17	0.05
LOI	0.18	0.32	0.30	0.82	0.66	0.32
Total	**99.24**	**99.10**	**99.28**	98.79	99.37	99.14
Li	9.00	12.00	25.00	11.00	41.00	9.00
Be	1.00	1.00	1.00	1.00	1.00	1.00
B	9.00	9.00	9.00	9.00	9.00	9.00
V	22.00	76.00	76.00	54.00	59.00	28.00
Cr	1349.00	150.00	217.00	73.00	64.00	119.00
Co	4.00	12.00	11.00	6.00	4.00	4.00
Ni	59.00	71.00	98.00	43.00	47.00	54.00
Cu	45.00	21.00	14.00	16.00	12.00	13.00
Zn	38.00	123.00	95.00	81.00	98.00	60.00
As	19.00	20.00	31,00	19.00	19.00	19.00
Rb	35.00	55.00	30.00	75.00	80.00	85.00
Sr	145.00	237.00	130.00	340.00	638.00	84.00
Y	22.00	61.00	24.00	105.00	28.00	43.00
Nb	19.00	35.00	21.00	21.00	20.00	19.00
Mo	4.00	4.00	4.00	4.00	4.00	4.00
Ag	0.90	0.90	0.90	0.90	0.90	0.90
Cd	1.00	1,00	1.00	1.00	1.00	1.00
Sn	19.00	19.00	19.00	19.00	19.00	19.00
Sb	9.00	9.00	9.00	9.00	9.00	9.00
Ba	729.00	712.00	301.00	807.00	1909.00	388.00
W	9.00	15.00	19.00	19.00	19.00	9.00
Pb	9.00	15.00	9.00	18.00	10.00	9.00

(Contd)

Table 2 : Normative Composition of the Orthogneiss from the Nunataks (Contd...)

	13/1-P2	25/1-ST8a	4/2-B1	6/2-ST5	7/2-B7	S/2-SN12
Bi	9.00	9.00	9.00	9.00	9.00	9.00
Zr	200.00	604.00	382.00	643.00	428.00	184.00
Th	11.00	3.00	12,00	0.21	16.00	5.70
Sc	7.30	18.00	21.00	15.00	12.00	14.00
Hf	5.10	28.00	11.00	32.00	22.00	6.90
Ta	0.13	0.72	0.55	0.97	0.01	0.40
La	45.00	58.00	46.00	108.00	150.00	28.00
Ce	90.00	113.00	88.00	184.'00	254.00	63.00
Nd	40.00	54.00	38.00	88.00	95.00	29.00
Sm	5.60	8.70	6.10	21.00	20.00	6.60
Eu	1.80	2.50	1.80	6.90	4.50	1.00
Tb	0.90	1.30	1.10	3.90	2.20	1.00
Yb	3.80	5.00	3.70	13.00	3.90	3.40
Lu	0.60	0.77	0.54	2.00	0.55	0.50
REETot	187.70	243.27	185.24	426.80	530.15	132.50
Q	33.15	22.66	26.22	25.14	19.93	27.10
c	0.10	1.18	1.17	2.90	0.59	0.00
Or	26.11	17.96	10.75	23.96	31.51	28.97
Ab	25.75	24.08	29.94	23.08	23.12	28.71
An	9.07	14.32	16.32	9.71	10.04	4.55
Ne	0.00	0.00	0.00	0.00	0.00	0.00
Lc	0.00	0.00	0.00	0.00	0.00	0.00
A	26.11	17.96	10.75	23.96	31.51	28.97
P	34.82	38.40	46.26	32.79	33.16	33.26
Ac	0.00	0.00	0.00	0.00	0.00	0.00
Ns	0.00	0.00	0.00	0.00	0.00	0.00
Di	0.00	0.00	0.00	0.00	0.00	2.98
DiWo	0.00	0.00	0.00	0.00	0.00	1.45
DiEn	0.00	0.00	0.00	0.00	0.00	0.40
DiFs	0.00	0.00	0.00	0.00	0.00	1.13
Hy	4.62	12.90	11.55	9.30	10.24	5.49
HyEn	1.33	3.99	3.34	2.94	3.50	1.43
HyFs	3.29	8.91	8.21	6.36	6.74	4.05
01	0.00	0.00	0.00	0.00	0.00	0.00
OIFo	0.00	0.00	0.00	0.00	0.00	0.00
OlFa	0.00	0.00	0.00	0.00	0.00	0.00
Mt	0.56	1.76	1.51	1.33	1.30	0.90
Hm	0.00	0.00	0.00	0.00	0.00	0.00
I I	0.46	3.40	2.17	2.95	2.22	0.92
Ap	0.15	1.61	0.33	1.52	0.98	0.35

resulting in the moderate to steep negative slope for the curves, indicating same degree of fractionation for both gneiss and charnockite. But the charnockites are relatively LREE-depleted than the gneisses which suggests the incompatibility of the LREE with respect to charnockite and the resultant partitioning of LREE in to the more granitic melt.

Discussion and Conclusion

In the variation diagrams of the orthogneiss and charnockite a clear trend of the progressive evolution of the charnockite and the gneiss from the parent magma is seen. This is further corroborated by the R_1-R_2 plot of Batchelor-Bowden (1985) wherein the charnockite which occurs as enclaves within the ortho-gneiss plot in the Pre-plate collision field while the host gneisses plot in the Syn-collision field (Fig. 14). The available REE data on

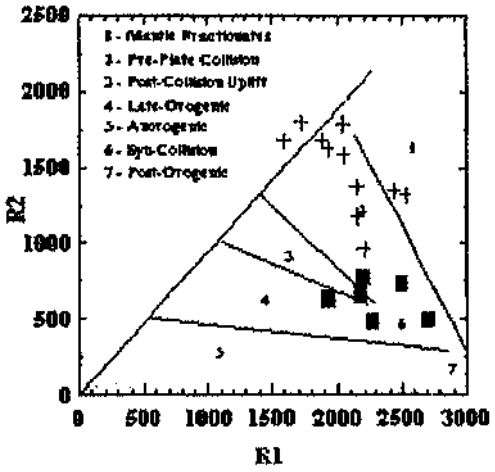

Fig. 14: R1R2 plot for the orthogneiss and charnockite which clearly indicates a pre-collision setting for the charnockite and a syn-collision setting for the orthogneiss

the gneisses of Schirmacher oasis (Srinivas, 1995) shows that the gneisses have low to moderate Total REE content (Σ REE = 19 - 218 ppm). These values are comparable to Σ REE of the charnockites (Σ = 17.62 - 216.69) of the nunataks while the gneisses are more enriched in Σ REE (Σ = 150.11-475.61). Further, the gneisses and charnockites of the nunataks are LREE enriched with respect to HREE as compared to the gneisses of Schirmacher, which have a relatively flatter REE pattern. It is also interesting to observe that the intrusion of lamprophyre dykes is more proliferate in the nunataks compared to Schirmacher. Whether this thermal event has got any role play

in resetting the REE profile in the gneiss and charnockite of the nunataks can only be speculative at this stage as data on chemistry of corresponding rock types in Schirmacher is awaited.

The geological set up of the four nunataks is quite interesting. In Baalsrudfjellet and Starheimtind nunataks, the orthogneisses alternate with the sillimanite-gneisses whereas in the other two nunataks, the sillimanite gneisses are conspicuously absent. A comparison with the distribution of such rock types in the Schirmacher Oasis, which lies just 20 km north of these nunataks, may throw some light. In Schirmacher, garnet-sillimanite gneisses occur in particular narrow zones (Fig. 15) in the west-central and eastern parts where ortho-gneiss (with all its variants) and garnet-sillimanite gneiss alternate. Since lithological set up in the nunataks is similar to that of Schirmacher and close proximity of these nunataks to Schirmacher, it is presumed that the nunataks are just extension of the Schirmacher Oasis. Thus the nunatak Pevikhornet and Sonstebynuten fall in the zones dominated by ortho-gneisses, while the nunataks Baalsrudfjellet and Starheimtind lie in the garnet- and garnet-sillimanite gneiss zone.

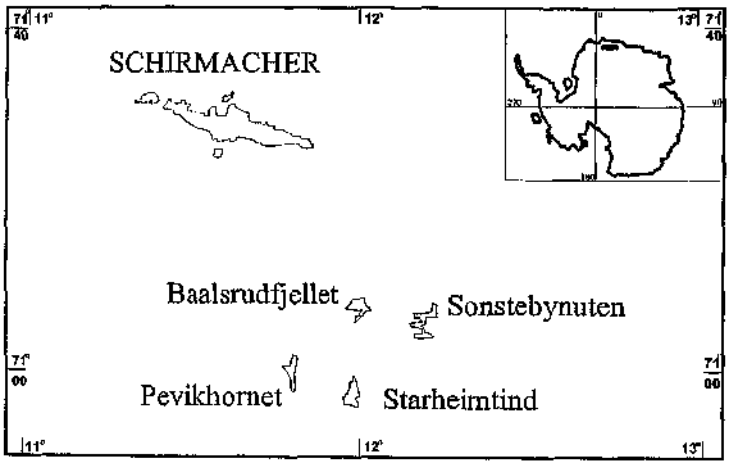

Fig. 15: Map showing zones in which garnet-sillimanite gneiss occurs; this probably explains the absence of pelitic gneiss in nunataks Pevikhornet and Sonsteby-nuten.

Acknowledgements

The authors are greatly indebted to Shri MK Kaul and Shri Rasik Ravindra, former and present Directors, respectively, of the Antarctica Division of GSI, Faridabad for their encouragement and support. The work was carried out in the 19th Indian Antarctic Expedition, under the aegis of NCAOR, Goa.

References

D'Souza MJ, Kundu A and Kaul MK (1996) The geology of a part of cDML, E. Antarctica. Ind. Min, 50 (4), pp 323-328.

Keshava Prasad AV, Beg MJ and Aran Chaturvedi (2001) Petrography of Lamprophyre dikes from nunataks southeast of Schumacher Oasis, cDML, E. Antarctica. Curr. Sci., 81(11), 2001, pp 1477-79.

Mukerji S, Kaul MK, Singh RK, Srivastava D and Jayaram S (1988) An outline of the geology of the nunataks between Eastern Wohlthat Ranges and Schirmacher Hills, Central Queen Maud Land, East Antarctica. DoD Tech. Publ. No 5, pp 121-133.

Srinivas Y (1995) Instrumental NAA of rock samples from Schirmacher range, cDML, E. Antarctica. DoD Tech. Publ. No 8, pp 137-144.

Tingey RJ (1991) The regional geology of Archaean and Proterozoic rocks of Antarctica pp 1-73. In 'The Geology of Antarctica' Ed. RJ Tingey, Oxford Science Publishers.